JETP Letters, Vol. 79, No. 11, 2004, pp. 532–536. From Pis'ma v Zhurnal Éksperimental'noĭ i Teoreticheskoĭ Fiziki, Vol. 79, No. 11, 2004, pp. 660–664.

Electronic Structure of Carbon Nanohorns near the Fermi Level¶

D. V. Kolesnikov and V. A. Osipov

Joint Institute for Nuclear Research, Bogolyubov Laboratory of Theoretical Physics, Dubna, Moscow region, 141980 Russia

e-mail: kolesnik@thsun1.jinr.ru; osipov@thsun1.jinr.ru

Received April 12, 2004

The effect of pentagonal defects on the electronic structure at the tip of carbon nanohorns is investigated within the continuum gauge field-theory model. It is found that the existence of a localized electron state at the Fermi level (a true zero-mode state) results in enhanced charge density near the tip. Using a self-consistent perturbation scheme, the eigenfunctions and the local density of states near the pentagonal defects are numerically calculated. © *2004 MAIK "Nauka/Interperiodica".*

PACS numbers: 73.22.-f

Nanohorns are novel synthesized members of a family of nanostructured carbon materials [1]. Experimentally [2], horn-shaped graphene sheets assemble to form dahlia flowerlike structures at the nanoscale. Some physical characteristics of nanohorns are unique, first of all, the prominent gas-adsorption phenomenon which makes it possible to use carbon nanohorns in fuel cells. It was also observed [3] that carbon nanohorn films have good field emission characteristics, making them promising candidates for field emission applications. It is interesting to note that the field amplification factor is found to depend on the geometrical shape of the emitter.

Geometrically, nanohorns are cone-shaped structures with a cone opening angle of about 19°, diameter of 2–4 nm, and length of about 50 nm [2]. Due to cone geometry, this opening angle corresponds to a 300° sector removed from the graphene sheet, which is equivalent to a creation of a $5\pi/3$ disclination. In turn, this means that nanohorns contain exactly five pentagons near the tip. Note, however, that the presence of the terminating cap at the tip of nanohorns does not allow the use of cone geometry for their description. In our opinion, a more appropriate geometry is the hyperboloid or, more precisely, the upper half of a two-sheet hyperboloid. Indeed, the hyperboloid has a cone asymptotic at large distances and a smoothing at the tip.

Both geometry and topological defects have a crucial influence on the electronic properties of carbon nanostructures. For instance, there is an important difference between electronic states at the apex of a cone and of a hyperboloid for the same number of pentagons. As was shown in [4], in the latter case, there is a possibility for the true zero-mode state. Namely, while for a cone normalized electron states at the Fermi level exist only for a finite system size and disappear in the infinite-size limit, they can exist for an infinite (full locus) hyperboloid. Likewise, a remarkable difference between electronic states near the tip of the pencil cap and bowl cap (containing six pentagons) was established [5] in metallic armchair nanotubes. At the same time, the different number of pentagons at the apex and even their relative location can lead to completely different behavior of electronic states [6–8].

The electronic properties of carbon nanohorns were theoretically studied in [6] using the parametrized linear combination of atomic orbitals (LCAO) technique. The optimum geometry and the electronic densities of states were determined for different nanohorn morphologies. This study shows that pentagonal sites determine all essential features of the electronic structure near the Fermi level at the tip. In particular, there appears negative excess charge near pentagons. It is interesting to study this problem within the continuum model. Despite the fact that the lattice disappears in the continuum description and, for example, nanohorns morphologies with different relative location of the five terminating pentagons cannot be taken into considerations, the continuum models were very effective in a study of electron states near the Fermi energy in fullerenes [9, 10], nanotubes [11], and nanocones [12, 13]. Moreover, the problem of specific electronic states at the Fermi level due to disclinations is similar to that of the fermion zero modes for planar systems in a magnetic field [14]. Generally, zero modes for fermions in topologically nontrivial background have been of current interest in both the field theory and condensed matter physics (see, e.g., review [15]). In addition, the continuum

¶ This article was submitted by the authors in English.

models allow us to study the electron states at large distances from the defects.

The first attempts to analyze the electronic states of carbon structures with a hyperboloid geometry within the continuum model were made in [4, 16]. The main finding was the existence of the normalized electron state at the Fermi level. However, any information about electronic states near the Fermi energy was lacking. In this paper, we adapt the continuum model to description of electronic states in nanohorns by considering the case of five pentagons at the tip (300° disclination) and taking into account a certain relation between the disclination power and the opening angle of the cone. Moreover, we develop a self-consistent perturbation scheme which allows us to calculate electronic eigenfunctions near the Fermi energy when the zero-mode solution is known. We also discuss asymptotic (long-range) solutions. Finally, we calculate the local density of electronic states (LDoS) near the Fermi energy.

Within the continuum approximation, we consider electrons on curved surfaces with disclinations taken into account. It was shown [17] that, for a flat graphene sheet, the self-consistent effective-mass theory can be reduced to the Dirac equation in (2 + 1) dimensions. This allows us to extend the consideration by formulating the Dirac equation on arbitrary curved surfaces incorporating topological defects by introducing $SO(2)$ gauge fields. In this context, disclination fields are accounted for by using the covariant derivative. As a result, the Dirac equation on an arbitrary surface in the presence of the $U(1)$ external gauge field W_μ is written as [10]

$$i\gamma^\alpha e_\alpha^\mu(\nabla_\mu - iW_\mu)\psi = E\psi, \qquad (1)$$

where ψ is a two-component spinor and γ_μ are the Dirac matrices which can be chosen to be the Pauli matrices: $\gamma^1 = -\sigma^2$, $\gamma^2 = \sigma^1$; $\nabla_\mu = \partial_\mu + \Omega_\mu$, with Ω_μ being the spin connection term and e_α^μ being the zweibein. The Fermi energy in (1) is chosen to be zero, so that the states at $E = 0$ are the well-known zero-mode states in the field-theory context. Notice that for massless fermions σ^3 serves as a conjugation matrix, and the energy eigenmodes in (1) are symmetric around $E = 0$ ($\sigma^3\psi_E = \psi_{-E}$). The gauge field W_μ determines an elastic flow through a surface which is given by a circular integral

$$\frac{1}{2\pi}\oint \mathbf{W}d\mathbf{r} = \nu,$$

where ν describes the topological characteristics of the defect (the Frank index). Due to the symmetry group of the hexagonal lattice, the possible values of the Frank index are multiplies of 1/6.

The eigenfunctions in (1) are classified with respect to the eigenvalues of $J_z = j + 1/2$, $j = 0, \pm1, \pm2, \ldots$, and are to be taken in the form

$$\psi = \begin{pmatrix} u(r)e^{i\varphi j} \\ v(r)e^{i\varphi(j+1)} \end{pmatrix}. \qquad (2)$$

Geometrically, the upper half of a hyperboloid can be regarded as the embedding

$$(\chi, \varphi) \longrightarrow (a\sinh\chi\cos\varphi, a\sinh\chi\sin\varphi, c\cosh\chi),$$
$$0 \le \chi < \infty, \quad 0 \le \varphi < 2\pi,$$

with a and c being the hyperboloid parameters. From this, the components of the induced metric can be obtained as (the details can be found in [4])

$$g_{\chi\chi} = \alpha^2\cosh^2\chi + c^2\sinh^2\chi,$$
$$g_{\varphi\varphi} = a^2\sinh^2\chi, \qquad (3)$$
$$g_{\varphi\chi} = g_{\chi\varphi} = 0,$$

which yields

$$\Gamma^\chi_{\chi\chi} = \frac{(a^2 + c^2)\sinh 2\chi}{2g_{\chi\chi}},$$
$$\Gamma^\chi_{\varphi\varphi} = -\frac{a^2\sinh 2\chi}{2g_{\chi\chi}}, \qquad (4)$$
$$\Gamma^\varphi_{\varphi\chi} = \Gamma^\varphi_{\chi\varphi} = \coth\chi$$

for the nonvanishing coefficients of the connection. In a rotating $SO(2)$ frame, the zweibeins take the form

$$e^1_\chi = \sqrt{g_{\chi\chi}}\cos\varphi, \quad e^2_\chi = \sqrt{g_{\chi\chi}}\sin\varphi,$$
$$e^1_\varphi = -a\sinh\chi\sin\varphi, \quad e^2_\varphi = a\sinh\chi\cos\varphi, \qquad (5)$$

which gives

$$\omega^{12}_\chi = \omega^{21}_\chi = 0, \ \omega^{12}_\varphi = -\omega^{21}_\varphi = \left[1 - \frac{a\cosh\chi}{\sqrt{g_{\chi\chi}}}\right] = 2\omega \qquad (6)$$

for the spin connection coefficients, so that

$$\Omega_\varphi = i\omega\sigma^3. \qquad (7)$$

The external gauge potential was found [4] to be $W_\chi = 0$, $W_\varphi = \nu$. In this case, the substitution

$$\tilde{\psi} = \psi\sqrt{\sinh\chi}$$

reduces eigenvalue problem (1) to the system of equations

$$\partial_\chi\tilde{u} = \sqrt{\coth^2\chi + b^2}\tilde{j}\tilde{u} = \tilde{E}\tilde{v},$$
$$-\partial_\chi\tilde{v} - \sqrt{\coth^2\chi + b^2}\tilde{j}\tilde{v} = \tilde{E}\tilde{u}, \qquad (8)$$

where $\tilde{E} = \sqrt{g_{\chi\chi}}E$, $b = c/a$, and $\tilde{j} = j - \nu + 1/2$.

Let us consider the zero-energy modes by setting $E = 0$ in (8). The general solution reads

$$\tilde{u}_0(\chi) = A\left[(k\cosh\chi + \Delta)^{2k}\frac{\Delta - \cosh\chi}{\Delta + \cosh\chi}\right]^{\tilde{j}/2},$$
$$\tilde{v}_0(\chi) = A\left[(k\cosh\chi + \Delta)^{2k}\frac{\Delta - \cosh\chi}{\Delta + \cosh\chi}\right]^{\tilde{j}/2}, \quad (9)$$

where $k = \sqrt{1 + b^2}$, $\Delta = \Delta(\chi) = \sqrt{1 + k^2\sinh^2\chi}$, and A is a normalization factor.

In the general case, for an unbounded hyperboloid (full locus), the normalization condition gives the following restrictions: $-1/2 < \tilde{j} < -1/2k$ for $u_0(\chi)$ and $1/2k < \tilde{j} < 1/2$ for $v_0(\chi)$. Thus, either $u_0(\chi)$ or $v_0(\chi)$ becomes normalizable on a hyperboloid of infinite volume except for the case $\nu = 1/2$. For $(c/a) \longrightarrow 0$, a normalizable solution does not exist. In fact, under this condition the hyperboloid is changing over to a plane. Consequently, our results are in accordance with the planar case.

Due to the cone asymptotic, it is quite reasonable to take into account the correspondence between the parameter k and the Frank index ν. Namely, like for a cone, one can specify $k = 1/(1 - \nu)$ (see, for example, [13]). In this case, only the $\tilde{u}_0$ mode becomes normalized and only for $j = 0$ and $3/4 < \nu < 1$. Therefore, a zero-mode solution exists for $\nu = 5/6$, that is, for the typical nanohorn configuration. This finding has an important physical consequence. Recall that there are two kinds of sublattice points in a unit cell of the graphene lattice due to degeneracy [17]. Hence, the presence of exactly one zero-mode state implies the enhancement of the electron densities only on one sort of points, while for two zero modes, both lattice points would have excess densities, thus allowing a metallization. Physically, this means that, for example, the field emission properties in the first case are less efficient. This agrees well with the experimental results in [3], where field emission properties of carbon nanohorn films were observed and compared with the best nanotube emitters.

The existence of zero-mode solutions allows us to formulate a self-consistent approximation procedure to obtain the eigenfunctions near the Fermi level. Namely, the substitution

$$\tilde{u}(\chi) = \tilde{u}_0(\chi)\mathcal{U}(\chi), \quad \tilde{v}(\chi) = \tilde{v}_0(\chi)\mathcal{V}(\chi)$$

reduces (8) to

$$\partial_\chi\mathcal{U} = \xi\Delta\mathcal{V}\frac{\tilde{v}_0}{\tilde{u}_0}, \quad \partial_\chi\mathcal{V} = -\xi\Delta\mathcal{U}\frac{\tilde{u}_0}{\tilde{v}_0}, \quad (10)$$

where $\xi = Ea$ or, in usual units, $\xi = Ea/\hbar v_F$ is a dimensionless parameter. For small ξ, $\mathcal{U}$ and $\mathcal{V}$ can be found by using the iteration procedure in the form

$$\mathcal{U} = \mathcal{U}^{(0)} + \xi\mathcal{U}^{(1)} + \ldots, \quad \mathcal{V} = \mathcal{V}^{(0)} + \xi\mathcal{V}^{(1)} + \ldots, \quad (11)$$

where $\mathcal{U}^{(0)}$ and $\mathcal{V}^{(0)}$ are constants, and

$$\mathcal{U}^{(1)}(\chi) = \mathcal{U}^{(1)}(0) + \mathcal{V}^{(0)}\int_0^\chi \Delta(\eta)\frac{\tilde{v}_0(\eta)}{\tilde{u}_0(\eta)}d\eta,$$
$$\mathcal{V}^{(1)}(\chi) = \mathcal{V}^{(1)}(0) - \mathcal{U}^{(0)}\int_0^\chi \Delta(\eta)\frac{\tilde{u}_0(\eta)}{\tilde{v}_0(\eta)}d\eta.$$

Notice also that this approximation is valid for sufficiently small χ (when $\xi\Delta \ll 1$) because $\Delta(\chi)$ is a rapidly increasing function in (10).

Before we proceed, let us discuss asymptotic solutions. At large distances, the hyperboloid geometry becomes nearly the same as the geometry of a cone. For large χ (when $\sqrt{g_{\chi\chi}} \gg a$), Eqs. (8) are written as

$$\partial_r\tilde{u} - (\tilde{j}k/r)\tilde{u} = Ek\tilde{v},$$
$$-\partial_r\tilde{v} - (\tilde{j}k/r)\tilde{v} = Ek\tilde{u}, \quad (12)$$

where $r = ae^\chi/2$, which is exactly the polar coordinate r introduced for the cone geometry in [12]. The exact solution to (12) reads

$$\tilde{u}_\infty = \sqrt{\frac{2r}{a}}\left(C_1 J_{\left|\tilde{j}k - \frac{1}{2}\right|}(Ekr) + C_2 J_{-\left|\tilde{j}k - \frac{1}{2}\right|}(Ekr)\right),$$
$$\tilde{v}_\infty = \sqrt{\frac{2r}{a}}\left(C_1 J_{\left|\tilde{j}k + \frac{1}{2}\right|}(Ekr) + C_2 J_{-\left|\tilde{j}k + \frac{1}{2}\right|}(Ekr)\right), \quad (13)$$

where $J_l(x)$ is the Bessel function and C_1 and C_2 are the constants. Naturally, when $r \longrightarrow \infty$ (13) can be approximated by

$$\tilde{u}_\infty \approx C\cos(Ekr + \varphi_0), \quad \tilde{v}_\infty \approx C\sin(Ekr + \varphi_0). \quad (14)$$

As follows from (14), $\tilde{u}_\infty^2 + \tilde{v}_\infty^2 \approx C^2 = \text{const}$, that is, the LDoS tends to a constant like for the cone (and like for a plane without disclinations). Notice that both Eqs. (12) and solutions (13) are also similar (but not identical) to those for a cone (cf. [4, 12]). Therefore, we may conclude that the influence of the disclination field on the density of states has a local character in the present geometry.

Since only one component in (9) becomes normalizable, one can set $\mathcal{V}^{(0)} = 0$ in (11). Then, in the leading approximation, one obtains

$$\tilde{u}(\chi) = \mathcal{U}^{(0)}\tilde{u}_0(\chi),$$
$$\tilde{v}(\chi) = -\xi\mathcal{U}^{(0)}\tilde{v}_0(\chi)\int_0^\chi \Delta(\eta)\frac{\tilde{u}_0(\eta)}{\tilde{v}_0(\eta)}d\eta. \quad (15)$$

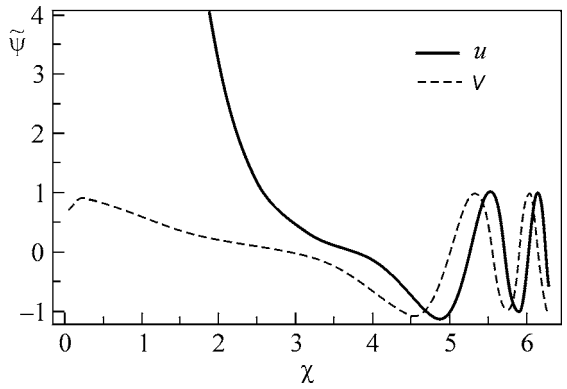

Fig. 1. The solution to (8) with the set of parameters $a = 1$, $j = 0$, $E = 0.01$, and $\nu = 5/6$.

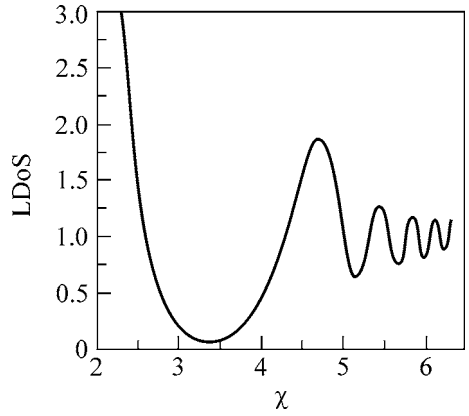

Fig. 2. Local density of states (per area) as a function of χ. The parameter set is the same as in Fig. 1.

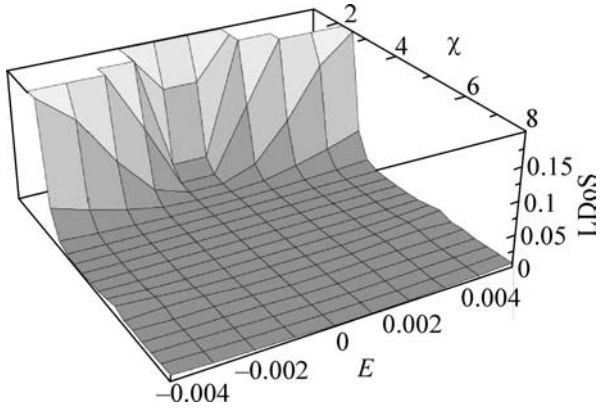

Fig. 3. Local density of states (per area) in arbitrary units as a function of χ and E. The parameter set (except E) is the same as in Fig. 1.

This allows us to integrate (8) numerically by using (15) as initial conditions. The results are shown in Figs. 1–3. As is seen from Fig. 1, the wave functions have an oscillatory behavior at large distances, in agreement with (14). With ξ decreasing, $\tilde{u}(\chi)$ rapidly increases while $\tilde{v}(\chi)$ decreases. Figure 2 shows the calculated LDoS (per area) as a function of χ at fixed energy. One can see a remarkable increase of the LDoS near the defect. The more detailed structure of the LDoS can be found in Fig. 3, where a 3D plot is presented. There is a finite density of electronic states at the Fermi level slowly growing with E.

Let us note once again that this behavior follows directly from the existence of the zero-mode state. For any other permissible values of the Frank indices (for a number of pentagons less than five), the zero mode does not exist and, correspondingly, no finite LDoS at the Fermi level is expected. It is interesting to compare our results with those obtained by the LCAO method [6], where only 25 atoms contained in the five terminating pentagons were considered for various tip morphologies. It is quite reasonable that the best agreement takes place for the most symmetrical arrangements of the pentagonal sites at the tip in [6]. Let us note also the good agreement of our results with [7] (at small E), where LDoS for five pentagons at the apex of a cone were investigated by using tight-binding calculations. In addition to [6, 7], the continuum description allows us to control the behavior of the LDoS at large distances from a tip which is linear in E, as for the flat graphene sheet.

To conclude, we have studied the electronic structure of carbon nanohorns within the continuum field-theory gauge model. The hyperboloid geometry is considered as the most appropriate for description of nanohorns. We have taken into account the natural correspondence between the parameters of the hyperboloid and the disclination power (the parameter k and the Frank index ν) and found that only for five pentagons at the tip does a normalized electron state appear at the Fermi level for an unbounded hyperboloid (the true zero-mode state). This finding allows us to formulate a self-consistent method for describing the electron states near the Fermi energy. The calculated LDoS rapidly grows in the tip region (near the disclination) and has a distinct nonzero minimum at the Fermi energy.

REFERENCES

1. S. Iijima, Physica B (Amsterdam) **323**, 1 (2002).
2. S. Iijima, M. Yudasaka, R. Yamada, *et al.*, Chem. Phys. Lett. **309**, 165 (1999).
3. J.-M. Bonard, R. Gaál, S. Garaj, *et al.*, J. Appl. Phys. **91**, 10107 (2002).
4. V. A. Osipov, E. A. Kochetov, and M. Pudlak, JETP **96**, 140 (2003).
5. T. Yaguchi and T. Ando, J. Phys. Soc. Jpn. **71**, 2224 (2002).

6. S. Berber, Y.-K. Kwon, and D. Tománek, Phys. Rev. B **62**, R2291 (2000).
7. J.-C. Charlier and G.-M. Rignanese, Phys. Rev. Lett. **86**, 5970 (2001).
8. P. E. Lammert and V. H. Crespi, Phys. Rev. B **69**, 035 406 (2004).
9. J. González, F. Guinea, and M. A. H. Vozmediano, Phys. Rev. Lett. **69**, 172 (1992); Nucl. Phys. B **406**, 771 (1993).
10. V. A. Osipov and E. A. Kochetov, JETP Lett. **72**, 199 (2000).
11. C. L. Kane and E. J. Mele, Phys. Rev. Lett. **78**, 1932 (1997).
12. P. E. Lammert and V. H. Crespi, Phys. Rev. Lett. **85**, 5190 (2000).
13. V. A. Osipov and E. A. Kochetov, JETP Lett. **73**, 562 (2001).
14. R. Jackiw, Phys. Rev. D **29**, 2375 (1984).
15. G. E. Volovik, Phys. Rep. **351**, 195 (2001).
16. R. Pincak and V. A. Osipov, Phys. Lett. A **314**, 315 (2003).
17. D. P. DiVincenzo and E. J. Mele, Phys. Rev. B **29**, 1685 (1984).